Macalester Journal of Physics and Astronomy

Volume 7
Issue 1 *Spring 2019*

Article 7

Binary Neutron Star Merger Rates. Predictions from Observations of Dwarf Galaxies and Observable Rates with Ground-Based Gravitational-Wave Detectors

Karen Perez Sarmiento
Macalester College, kperezsa@macalester.edu

Abstract

Binary Neutron Star (BNS) mergers are interesting events in the field of multi-messenger astronomy since they are sources of detectable gravitational wave signals and electromagnetic transients. Here I introduce a new method to calculate a conservative, lower-limit for the rate of BNS merger events that is proportional to the stellar mass and is based on evidence of an r-process event in the dwarf galaxy Reticulum II. Two estimates of the stellar mass in the nearby universe were made using a Schechter Mass Function and a modified version of the 2MASS Extended Source Catalog (2MASS XSC). The BNS merger event rates were calculated to be 285.88 and 266.77 $Gpc^{-3}yr^{-1}$ from the Schechter Mass Function and the galaxy catalog mass estimates, respectively. Predictions of observed rates with LIGO were made considering that ground-based gravitational-wave detectors have preferential sensitivity dependent on right ascension and declination. The predicted observed rate for a 200 Mpc volume was estimated at 6.30 yr^{-1}. Additionally, this work explored other uses of the galaxy catalog created to estimate the rate BNS mergers, such as in the identification of the source galaxy during observation campaigns of these events, and in cosmological parameter estimation.

Binary Neutron Star Merger Rates.

Predictions from Observations of Dwarf Galaxies and Observable Rates with Ground-Based Gravitational-Wave Detectors.

Karen Perez Sarmiento

Macalester College, Department of Physics and Astronomy

May 11, 2019

Abstract

Binary Neutron Star (BNS) mergers are interesting events in the field of multi-messenger astronomy since they are sources of detectable gravitational wave signals and electromagnetic transients. Here I introduce a new method to calculate a conservative, lower-limit for the rate of BNS merger events that is proportional to the stellar mass, and is based on evidence of an r-process event in the dwarf galaxy Reticulum II. Two estimates of the stellar mass in the nearby universe were made using a Schechter Mass Function and a modified version of the 2MASS Extended Source Catalog (2MASS XSC). The BNS merger event rates were calculated to be 285.88 and 266.77 $\mathrm{Gpc}^{-3}\mathrm{yr}^{-1}$ from the Schechter Mass Function and the galaxy catalog mass estimates, respectively. Predictions of observed rates with LIGO were made considering that ground-based gravitational-wave detectors have preferential sensitivity dependent on right ascension and declination. The predicted observed rate for a 200 Mpc volume was estimated at 6.30 yr^{-1}. Additionally, this work explored other uses of the galaxy catalog created to estimate the rate BNS mergers, such as in the identification of the source galaxy during observation campaigns of these events, and in cosmological parameter estimation.

1 Background

1.1 Binary Neutron Star Mergers: current model

Binary Neutron Stars (BNS) are gravitationally bound systems of two neutron stars that merge through a process called inspiral. There are thousands of known Neutron Stars but only about 70 are found in

binary systems. BNS systems emit gravitational waves as they orbit each other, which causes the orbital distance to decrease as the frequency of the emitted waveforms increases (Rasio and Shapiro 1999). For many years, they were considered the most promising sources of gravitational waves, yet the first two observing runs of the Laser Interferometer Gravitational Wave Observatory (LIGO) failed at detecting any event. Instead, LIGO detected several Binary Black Hole (BBH) merger events before the first detection of a Binary Neutron Star event.

In addition to gravitational-wave signals, existing models for electromagnetic signatures from BNS mergers predict three types of transients (Metzger and Berger 2012). The first are Short Gamma Ray Bursts (SRGBs), which are short ($<$ 2seconds), non-repeating, intense flashes of relativistic photons (Berger 2014). Berger (2014) proposed that the clear short-long duration divide in gamma-ray bursts pointed to two different types of progenitors. While long gamma-ray bursts have been associated with Type Ic supernovae, compact object binaries have long been proposed as the progenitors for short gamma-ray bursts. Moreover, evidence of SGRB occurrence in early-type, elliptical galaxies points to old stellar population progenitors, whereas long gamma-ray bursts only occur in star-forming galaxies (Berger 2014).

Due to the association between SGRBs and compact object coalescence events, many predictions on the astrophysical rates of BNS merger events were based off SGRB rates (Petrillo et al. 2013). However, this methodology introduces some challenges since SGRBs can only be observed at certain angles because their energy is emitted in a cone shape. The half-opening angle (half of the angle of the cone) defines the portion of the sky in which we can observe them but current observations and models propose a wide range of angles.

Moreover, another issue with estimating BNS merger rates from SGRBs is that it is not certain there is a one-to-one correspondence between both types of events. It is possible that a fraction of SGRB progenitors are compact object mergers other than BNSs, and it is also possible that not all BNS mergers produce SGRBs. By assuming that 85% of all SGRBs come from BNS merger events and adopting an average half-opening angle of $\theta = 20^{\circ}$, Petrillo et al. (2013) estimated rates of BNS mergers ranging from 479 to 1025 $\mathrm{Gpc}^{-3}\mathrm{yr}^{-1}$. These rates, however, are highly sensitive to opening angle. Fong et al. (2015) estimated the true SGRB rate at $270^{1580}_{180}\mathrm{Gpc}^{-3}\mathrm{yr}^{-1}$. Thus, predictions of rates from SGRB are highly dependent on the uncertain geometry of these events, which results in estimated rates ranging several orders of magnitude.

Another electromagnetic signature of BNS mergers, directly associated with Short Gamma Ray Bursts, is the afterglow, visible at optical and radio wavelengths in timescales of days to weeks, respectively.

The third electromagnetic signature predicted from BNS mergers are kilonovae. Kilonovae are isotropic emissions triggered by the decay of radioactive elements, and are expected to be observable on timescales of about 1 day. Metzger et al. (2010) distinguishes a kilonova from a Type 1a supernova

based off the ejecta material: the former produces neutron rich material while the latter mostly ejects ^{56}Ni. Moreover, the duration of kilonovae are estimated to be much shorter than that of supernovae, and the energy released in the transient lower (Metzger et al. 2010). Decompression of the merger ejecta allows the formation of heavier radioactive elements through r-process nucleosynthesis (Doctor et al. 2017), and the resulting beta decay may be detectable at optical/near-IR wavelengths (Berger 2014).

R-process nucleosynthesis, or rapid-neutron capture nucleosynthesis, consists on the capture of neutrons by nuclei in timescales shorter than the half-lifetime of the corresponding beta decay, thus resulting in neutron-rich nuclei. R-process events produce a distinct pattern for the chemical abundance of heavy elements.

Given the fast evolution of BNS electromagnetic transients, the most likely strategy for their detection is by following-up gravitational-wave detections. Nevertheless, this strategy also presents challenges since only telescopes with sufficient depths, sensitivities, cadence, and field of views can in principle participate in the search of electromagnetic counterparts following a gravitational-wave trigger (Metzger et al. 2010). Large survey telescopes, as well as optical transient surveys, such as the Palomar Transient Factory and the Large Synoptic Survey Telescope, are expected to be key participants in the electromagnetic follow-up of gravitational-wave events. In the following section, the electromagnetic follow-up of GW170817 is described to exemplify the current strategies in place and pinpoint challenges to be overcome before LIGO's next observing run.

1.2 Event GW170817

On August 17th, 2017, the possible merging of a Binary Neutron Star was reported by the Advanced LIGO and Advanced Virgo detectors. The gravitational-wave signal triggered a worldwide observation campaign to search for the location of the electromagnetic transient in the sky and observe it across all wavelengths of the electromagnetic spectrum (Abbott et al. 2017). Shortly after the single-detector trigger of a potential gravitational-wave signal, analysis of the data from the three gravitational-wave observatories confirmed a significant coincident signal and were able to produce a localization map of the source in a region of 31 deg^2 around 12h57m, -17°51', and at a distance of about 40 Mpc. The masses of the primary and secondary components were estimated at $m_1 = (1.36 - 2.26)M_\odot$ and $m_2 = (0.86 - 1.36)M_\odot$, while the chirp mass was measured to be $M = 1.188^{+0.004}_{-0.001}M_\odot$. Moreover, since the gravitational-wave signal was observed at frequencies of about 200 Hz, this constrained the size of the orbit to about 100 km. Both the small size of orbit as well as the the low component and chirp mass indicated that the merger was due to objects more compact than a white dwarf (Abbott et al. 2017).

Meanwhile, after initial notice from the LIGO-Virgo collaboration of a possible gravitational-wave event, the Fermi Gamma-Ray Burst Monitor detected a short gamma-ray burst within 2 seconds of the gravitational-wave signal, the event now referred to a GRB170817A. Fermi-GBM reported a 90%

localization probability region centered at around 12h28m,-30º of area 1100 deg^2. This area was later constrained by the detection of the SGRB with the detector INTEGRAL SPI-ACS (Abbott et al. 2017).

The duration of the burst was estimated at about $2 \pm 0.5s$ Given the temporal coincidence with the independent detection of a gravitational-wave signal by the Advanced LIGO observatories, the LIGO-Virgo AND Fermi GBM collaborations issued a circular to the astrophysics community, and thus began the campaign to localize and observe the transient. The optical transient only became observable in the northern hemisphere about 10 hrs after the gravitational-wave detection, during the western hemisphere nightime. Many collaborations around the globe joined the campaign to localize the event, and the first one to do so was the One-Meter, Two-Hemisphere team with the 1 m Swope telescope in Chile. The transient was localized at $\alpha(J2000.0) = 13^h09^m48.085^s$, $\delta(J2000.0) = -2322'53.343'']$ near the galaxy NGC 4993. The known distance to this galaxy is 40 Mpc, which was consistent with distance estimates provided by the gravitational wave observatories (Abbott et al. 2017).

Within an hour, other teams also located the optical counterpart, and over the next weeks, the transient was observed in UV, optical and near-infrared observatories. Continuous observations of the object showed a rapid dimming in UV-blue emission, followed by optical red and near-infrared dimming within the next few days. The unusual fast decay in luminosity in a matter of days was indicative of the unprecedented nature of the transient. Spectroscopic observations were also key in distinguishing the nature of the transient from other more common cataclysmic events, such as core-collapse supernovae. Spectra of the transient showed a featureless blue continuum with rapid fading (Abbott et al. 2017). These observations strongly suggested that the transient object under consideration could not be attributed to supernova, but instead was qualitatively consistent with known models of kilonova.

1.3 The Ultra-Faint Dwarf Galaxy Reticulum II

Reticulum II (Ret II) is an ultra-faint dwarf galaxy (UFD) in the local group recently discovered in the first year of the Dark Energy Survey (DES-Y1). Roederer et al. (2016b) and Ji et al. (2016) performed high-resolution spectroscopic analysis on nine Ret II members and reported their chemical abundance pattern. Seven of those stars follow the universal r-process pattern for elements above Ba and the discrepancy for lighter elements may be explained by an universal r-process pattern that does not extend to light r-process elements. There are several proposed mechanisms for the site of the r-process Ret II. A core-collapse supernova event is one of the proposed production sites for r-process. Nevertheless, the [Eu/Fe] abundances in Ret II are the highest found in any UFDs and about 1000 times higher than the typical yields of supernovae. This points out to a rare, single progenitor for the enhanced r-process element abundances found in Ret II (Ji et al. 2016a). In fact, the most promising site for the r-process enhancement in this galaxy is a kilonova resulting from a BNS merger since they are predicted to readily produce high abundances of r-process elements.

Table 1: Properties of Reticulum II.

α_{2000} (deg)	δ_{200} (deg)	Distance (kpc)	$\log_{10}(\tau)$ $\log_{10}(Gyr)$	Z
53.92	-54.05	32	10.08 $\pm$0.21	0.0003

1.4 Gravitational-wave observations of compact objects and cosmology

Gravitational-wave signals, along with their electromagnetic counterparts, can be used to independently calculate cosmological parameters. In a manner similar to how supernovae are used as standard candles to measure distances in the universe, joint detections of gravitational waves and electromagnetic signals can also be used as standard sirens for cosmology studies (Holz and Hughes, 2005). Parting from the assumption that general relativity describes the waveform of the gravitational-wave signal observed, if we also have an independent redshift measure of the source, it is then possible to constrain several cosmological parameters, such as the Hubble constant, the dark energy equation of state parameter, the average density of matter and dark energy. There exists a discrepancy between Planck satellite Hubble constant measurement ($67.4 \pm 1.4 \mathrm{kms}^{-1}\mathrm{Mpc}^{-1}$) and those from distance ladder studies (74.3 ± 1.5km $\mathrm{s}^{-1}\mathrm{Mpc}^{-1}$). In this sense, cosmological parameter estimation from standard sirens will offer a different set of systematics from which to compare other methods. Standard siren calculations rely on the luminosity distance-redshift relation, which depends on the Hubble parameter, the Hubble constant and redshift.

At low redshifts, such as in the realm of observable binary neutron star mergers with current gravitational wave observatories, the distance-redshift relation simplifies to:

$$D_L = \frac{cz}{H_0} \tag{1}$$

The gravitational waveform signal contains information about the binary's luminosity distance D_L, its position in the sky, the redshifted chirp mass M_z and the redshifted reduced mass μ_z. Nevertheless, the gravitational waveform does not provide direct information about the source redshift. Thus, in order to complete the distance-redshift relation, and independent measure of the redshift is required. There are several methods to calculate the source's redshift, and one of these options is to use existing galaxy catalogs.

The posterior probability density function of H_0 given a set of measurements obtained through gravitational-wave and electromagnetic observations depends on computing the likelihood of observing a gravitational-wave signal given a Hubble constant, a redshift distribution for the event, the observed electromagnetic redshift, and a set of parameters for the event (such as binary masses and sky position angle). This likelihood can be calculated using a Metropolis-Hastings Markov Chain Monte-Carlo (MCMC) method. Nissanke et al. (2010) applied this method to an artificially generated set of detectable binary neutron star mergers with identifiable electromagnetic counterparts. The joint posterior

probability distribution of H_0 narrows down as the number of detected events increases. Moreover, the error in the computed value of H_0 also decreases as more detectors join the network of gravitational-wave observatories since this will allow for even more detections of gravitational-wave events. Nissanke et al. (2010) predict that about 20-30 GW-EM events are needed to accurately measure H_0 down to a percent level accuracy, competitive with existing estimates computed with other methods.

2 Methods

2.1 Calculation of a conservative, lower limit to the rate of BNS mergers

The r-process enhancement present in Ret II, and the evidence for a rare, prolific, single event as its progenitor, strongly suggests that a BNS merger occurred in this galaxy. High-resolution spectroscopic analyses performed in another 12 dwarf galaxies show very low abundances of neutron-capture elements and therefore no evidence of prolific r-process events (Ji et al. 2016a). In this context, the candidate BNS merger event in Reticulum II can be used as the basis to calculate a conservative lower estimate to the rate of these events.

From the composite stellar mass of these 13 dwarf galaxies and by placing an upper limit to the timescale of the r-process event in Ret II, we built a simple rate calculation of BNS mergers that is assumed to scale up with stellar mass. The formula is as follows:

$$R_{BNS} = \frac{1 event}{\sum_i^{13} M_* \times (T_{universe} - T_{event})} = 10^{-15} M_\odot^{-1} yr^{-1} \quad (2)$$

The motivation for using the stellar mass of the galaxies as the characteristic property for the rate of BNS merger events arises from the fact that it is the simplest property associated with the number of neutron stars formed within a galaxy. There is no reason to believe Ret II conforms to a particular environment that enhances the existence of BNS systems and the occurrence of mergers. The fact that there is no evidence of r-process enhancement events in any of the other UFDs with known metal abundances places Ret II more on the exception than the norm. Therefore, the safest assumption is that the rate of BNS mergers scales up with galactic stellar mass. Moreover, stellar mass can easily be derived from direct observable properties, such as absolute magnitude. A BNS rate that solely depends on the stellar mass is an oversimplification. Some of the caveats of this assumption include the fact that initial mass functions are not the same for all the galaxies, nor are star formation rates in different types of galaxies. The upper limit for the timescale of the r-process event was set to the age of the universe minus the stellar population age of Ret II, which was calculated by fitting an isochrone to the color distribution of the stars ($\tau = 13.5$ Gyr) (Bechtol et al. 2015).

The method proposed in this work is independent on any assumptions of SGRBs, which are the typical signatures employed in the literature to estimate rates of BNS mergers. SGRBs are associated with a beaming angle, for which observable rates require correction factors that account for the number of unobserved events (Coward et al. 2012; Fong et al. 2015; Chen and Holz 2012). Moreover, it is not established whether the sole progenitors of SGRBs are BNS mergers or if all BNS mergers result in SGRBs signatures. In this sense, agreement between BNS merger rates calculated with different methods and beam-corrected SGRB rates could provide stronger evidence for the current model of the electromagnetic signatures of BNS mergers.

Table 2 states the stellar masses of the 13 Dwarf galaxies considered in the BNS merger rate calculation above.

Table 2: List of the 13 Dwarf Galaxies with High-resolution spectroscopic analysis and their stellar masses.

Name	M_* $[10^3 M_\odot]$	Source
Ret II	2.6	Bechtol et al. (2015)
Hor I	2.4	Bechtol et al. (2015)
Tuc II	3	Bechtol et al. (2015)
Tuc III	0.8	Drlica-Wagner et al. (2016)
Boo I	29	McConnachie (2012)
Boo II	1	McConnachie (2012)
ComBer	3.7	McConnachie (2012)
CVnII	7.9	McConnachie (2012)
Her	37	McConnachie (2012)
Segue 1	0.34	McConnachie (2012)
Segue 2	0.86	McConnachie (2012)
UMa II	4	McConnachie (2012)
Leo IV	19	McConnachie (2012)

2.2 Estimations of Stellar Mass in the nearby universe

From the previous formalism that assumes the rate of BNS mergers to be proportional to galactic stellar mass, we can obtain astrophysical rates for these events within the observable range of LIGO by estimating the stellar mass contained in a given volume. Two methods were employed for such estimation: a variation of the Schechter Mass Function integrated over a range of galactic stellar masses, and a modified version of the 2MASS XSC (complete to J$<$ 15) that covers the whole sky and includes properties such as the JHK magnitudes and distances for each object. Results from both methods can then be compared with each other to ensure reliability of the stellar mass estimates.

2.2.1 Schechter Mass Function approach

The Schechter Mass Function is an analytic approximation of the space density of galaxies as a function of their stellar mass (Schechter 1976). It was first derived as a luminosity function and exhibits the

behavior of a power law. The formula is as follows:

$$\phi(M) = b \times \phi^* \ln(10)[10^{b(M-M^*)}]^{(1+\alpha)} \exp[-10^{b(M-M^*)}] \quad (3)$$

In this function, $b = 1$ for the mass function, M^* is the characteristic mass in log units and determines where the mass function changes slope, and M is the mass in log units. ϕ^* is the normalization and α determines the slope for fainter galaxies. Values for the parameters as a function of redshift were derived by Conselice et al. (2016). They were calculated by fitting the Schechter function to galaxy surveys and catalogs at different redshifts for a standard cosmology of $H_0 = 70\text{kms}^{-1}$, and $\Omega_m = 1 - \Omega_\Lambda = 0.3$. For the purposes of this paper, we used the parameters for the lowest redshift bin available (0.2<z<0.4): $\alpha = -1.19; \quad \log M^* = 11.20 M_\odot; \quad \phi = 22.4 \times 10^{-4}\text{Mpc}^{-3}$. One of the caveats of this formalism is the fact that we do not know the exact lower limit for which the function remains valid. Conselice et al. (2016) recommended a fiducial $M_* > 10^6 M_\odot$ lower limit, since that is the typical lower limit for dwarf galaxies in the nearby universe. The function as stated calculates the number of galaxies of a given mass in a 1 Mpc^3 volume. We can calculate the stellar mass from the space density of galaxies by multiplying the Schechter Mass Function by 10^M and integrating over the ranges $10^6 M_\odot$ to $10^{12} M_\odot$. The limits of integration were chosen from the fiducial lower mass limit of the formula and the typical sizes for the largest galaxies. The estimated stellar mass in 1 Gpc^3 volume from the Schechter formalism yields a stellar mass of $4.09 \times 10^{17} M_\odot$.

2.2.2 The Galaxy Catalog approach

The 2MASS Extended Source Catalog reports right ascension, declination, and J, H, and K apparent magnitudes. It was complemented with distance values, calculated from photometric and spectroscopy redshifts as well as distance moduli values from several other galaxy catalogs since no single catalog was able to populate the entire distance column. Distances from distance moduli took preference, followed by spectroscopic redshifts, and finally photometric redshifts. We adopted a standard cosmology of $H_0 = 70\text{kms}^{-1}$ and $\Omega_m = 0.3$. Below is a summary of the process followed to populate the distance column and the specific galaxy catalogs used in each step:

a) The highest preference was given to distances calculated from distance moduli values stated in the EDD/Cosmicflows2 catalog.

b) Second degree of preference was given to distances calculated from the distance moduli values in NED catalog.

c) Next, distances calculated from SDSS spectroscopic redshifts were considered.

d) NEDZ spectroscopic redshifts took the following degree of preference.

e) Finally, for the remaining objects without distance values, distances from the 2MPZ photometric redshifts were considered.

Of the 1646844 objects in the original version of the 2MASS XSC, a total of 612837 were matched to at least one distance proxy. Table 3 shows the number and percentage of distance values that were calculated from distance moduli, spectroscopic, and photometric redshifts. Percentages were calculated from the total number of objects with at least one distance match.

Masses for each object were calculated using a mass-to-light ratio relation with J-K color (Westmeier et al. 2011; Bell and de Jong, 2001).

$$\log \frac{M/M_{\odot}}{L_K/L_{\odot,K}} = 1.434(J-K) - 1.380 \tag{4}$$

$$\frac{M}{M_{\odot}} = 10^{1.434(J-K)-1.380+0.4(M_{\odot,K}-M_K)} \tag{5}$$

Where the absolute magnitude of the sun in K-band is $M_{\odot,K} = 3.28$, and M_K is the absolute magnitude of the object also in K-band.

Table 3: Distance column composition of modified version of 2MASS XSC.

Type	Number of sources	Percentage
Distance Moduli	11778	1.92
Spectroscopic redshifts	287013	46.83
Photometric redshifts	314046	51.24

The following plot shows the integrated stellar mass per pixel of the modified version of the 2MASS XSC up to a distance of 200 Mpc.

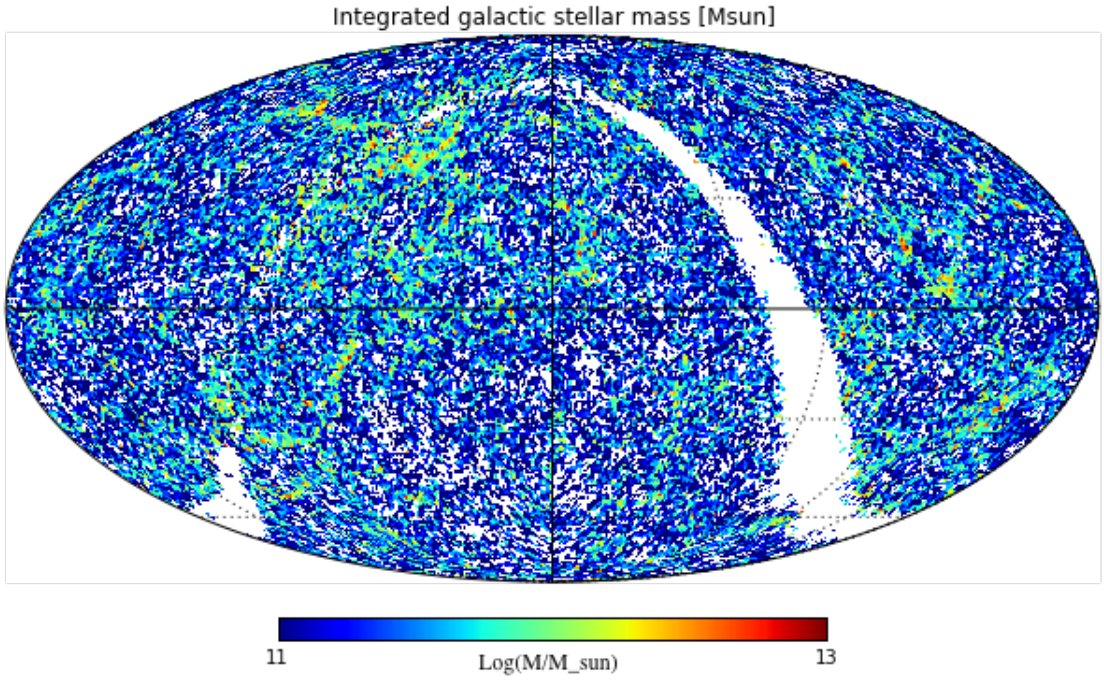

Figure 1: Integrated stellar mass $[M_{\odot}]$ per pixel as calculated from equation 4 for a radius of 200 Mpc. Stellar masses of objects $M_* > 5 * 10^{12}$ were removed from catalog.

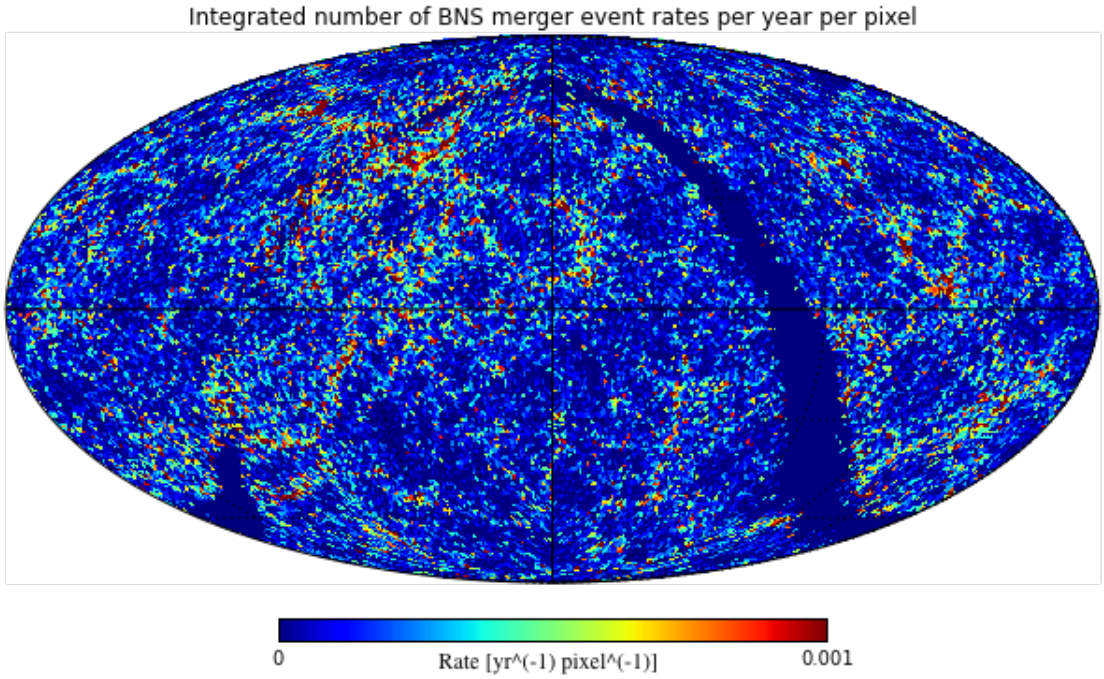

Figure 2: Integrated BNS merger rates per pixel up to a distance of 200 Mpc as calculated from equation 1 and the integrated stellar mass map in figure 1.

From Figure 1, it is possible to match the overdense regions in the map with known galaxy clusters, i.e. the Coma Cluster and the Virgo Supercluster.

3 Results

Figure 2 shows the integrated BNS merger rates per pixel up to a distance of 200 Mpc as calculated from the integrated stellar masses per pixel from figure 1.

The total integrated stellar mass for a 200 Mpc volume as estimated by the galaxy catalog is $1.28 \times 10^{16} M_{\odot}$. We integrated the stellar mass in distance bins from 0 to 200 Mpc in increments of 20 Mpc, in order to calculate rates at those specific distances. BNS merger rates were also calculated from the Schechter formalism by scaling up the estimated stellar mass in 1 Mpc^3 for radii ranging from 0 to 200 Mpc.

In order to predict the number of observable BNS merger events with LIGO, the observational selection effects of the GW observatory discussed in the introduction must be taken into account. We used monthly maps of LIGO's sensitivity pattern taken from Chen et al. (2017), and multiplied them by the integrated BNS merger rate map created with the galaxy catalog to obtain individual monthly and composite year predictions for the number of observable events with LIGO. We assumed LIGO's sensitivity to be independent from distance, which is not the case given that . Nevertheless, future LIGO

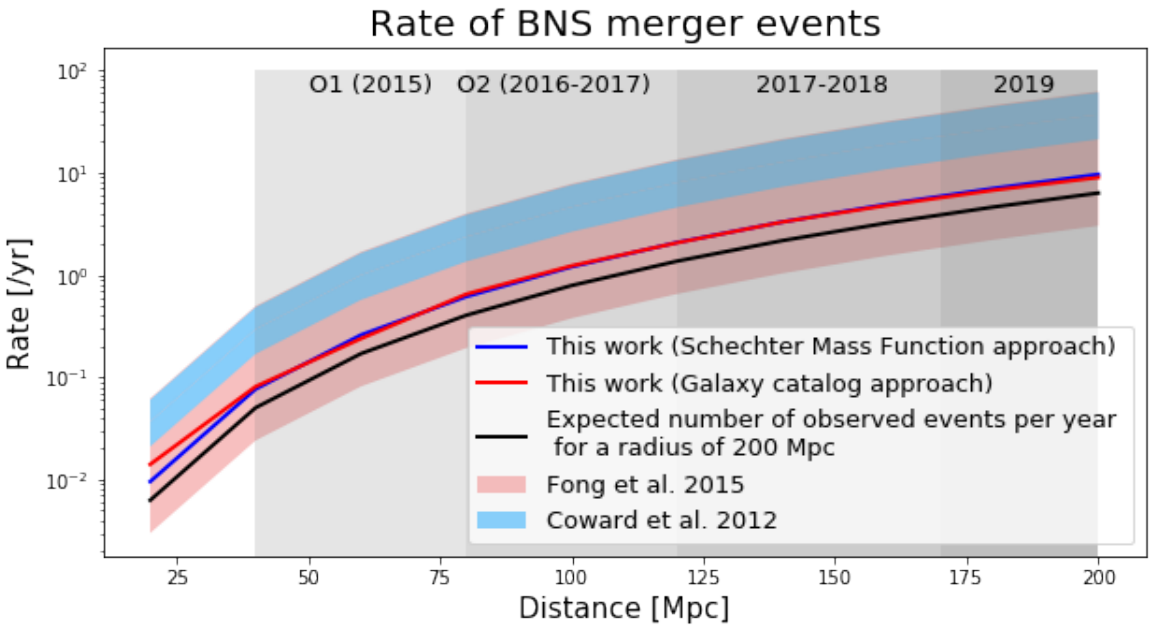

Figure 3: BNS merger rates for different radial distances calculated based on two independent estimates of the stellar mass in the nearby universe, and observable rates with LIGO, as compared to SGRBs rates reported in the literature. Rates are shown for the scales of LIGO's range in past, present, and upcoming observing runs.

upgrades are in place to push its sensitivity up to 200 Mpc. By using this method, we calculated an observable BNS merger rate of $6.3\mathrm{yr}^{-1}$ for a 200 Mpc radius.

Moreover, we performed a literature search of SGRBs beam-corrected rates. Fong et al. (2015) predicted a beam-corrected rate of $R_{true} = 270^{+1580}_{-180}\mathrm{Gpc}^{-3}\mathrm{yr}^{-1}$ from analysis of broadband afterglow and opening angle measurements of a SGRB catalog. Coward et al. (2012) also predicted both a SGRB lower rate density of $R_{lower} = 8^{+5}_{-3}\mathrm{Gpc}^{-3}\mathrm{yr}^{-1}$ and a beaming corrected upper limit of $R_{upper} = 1100^{+700}_{-470}\mathrm{Gpc}^{-3}\mathrm{yr}^{-1}$, accounting for the dominant bias in the sample of SGRBs with reasonably firm redshifts. Figure 3 shows the BNS merger rates calculated with the Schechter formalism approach, the galaxy catalog approach, and the observable rate considering LIGO's nonuniform sensitivity. These rates are compared to SGRB rates reported in Fong et al. (2015) and Coward et al. (2012).

From the plot we can see that there is very good agreement between the rates calculated with the Schechter Function and the rates from the Galaxy Catalog for nearly every distance. This gives us confidence in the two independent methods we used to estimate the stellar mass in the nearby universe.

Moreover, it is important to notice that our BNS merger rates are within the range of lower limits proposed by Coward et al. (2012) and Fong et. al (2015). The general agreement between SGRB literature rates and the BNS merger rates calculated through our independent method based on the r-process event in Ret II points to the close relation between BNS merger rates and SGRBs beyond theoretical models.

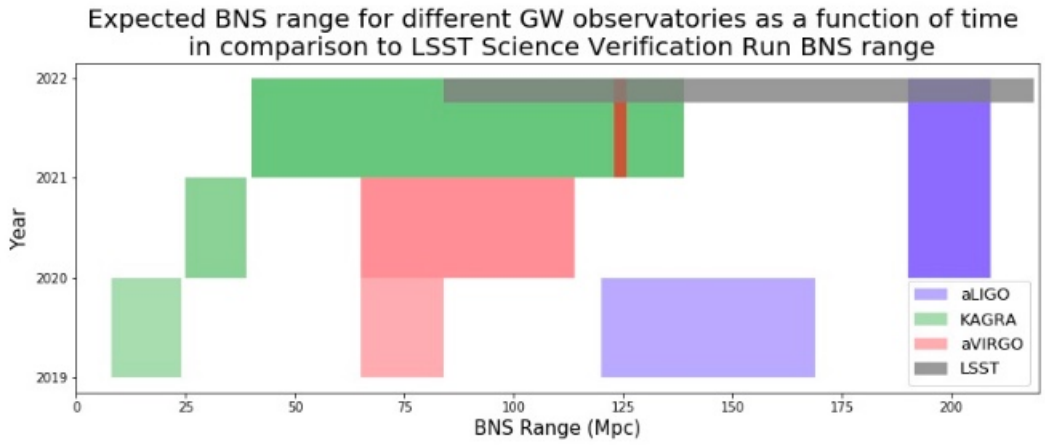

Figure 4: BNS range of GW observatories is dependent on the sensitivity of the detectors. aLIGO and aVirgo will run at design sensitivity by 2021, while KAGRA will run at late phase sensitivity.

3.1 Prospects of observing BNS merger events with LSST

The Large Synoptic Sky Telescope (LSST), with its ample sky coverage and unprecedented depth, is expected to become one of the leading tools for the electromagnetic follow-up of GW signals from BNS mergers. This section presents the prospects of observing such events during the LSST Science Verification run, scheduled for late 2021. These predictions account for the expected sensitivity that current detectors (aLIGO and aVirgo), as well as future GW observatories (KAGRA) will reach by 2021.

The LSST Science Validation (SV) run is scheduled for the third and fourth quarter of 2021. It will consist of two intercalated surveys: Survey 1 (Wide Area) and Survey 2 (10 year depth).

-Survey 1: Wide Area: 1600 $\deg^2$ x 15 visits x 2 phases. Phase 1: Observations for template generation (20 nights). Phase 2: Observation of same area for alert production (20 nights)

-Survey 2: 10-yr depth: 300 $\deg^2$ x 825 visits across 6 filters. Data release products at full survey depth. Data quality characterization beyond the SRD.

LSST has two survey strategies Wide Fast Depth (WFD), and Deep Drilling Fields (DDF). The WFD survey has a design depth of 24.5 in r-band, whereas for DDF it is 25.6. Survey 2 of the Science Verification run is supposed to reach the design depth of the WFD strategy. The Kilonova redshift range for LSST WFD, as calculated from simulated lightcurves in Scolnic et al. 2017, is 0.02 - 0.25. These redshifts correspond to an 84 - 1000 Mpc range.

By 2021, Advanced LIGO (aLIGO) is predicted to reach a BNS range of 190 - 210 Mpc, Advanced Virgo (aVirgo) 125 Mpc, and KAGRA, currently under construction in Japan, is schedule to reach a BNS range of 40-140 Mpc.

The observation and identification of BNS events with LSST will be constrained by the sensitivity

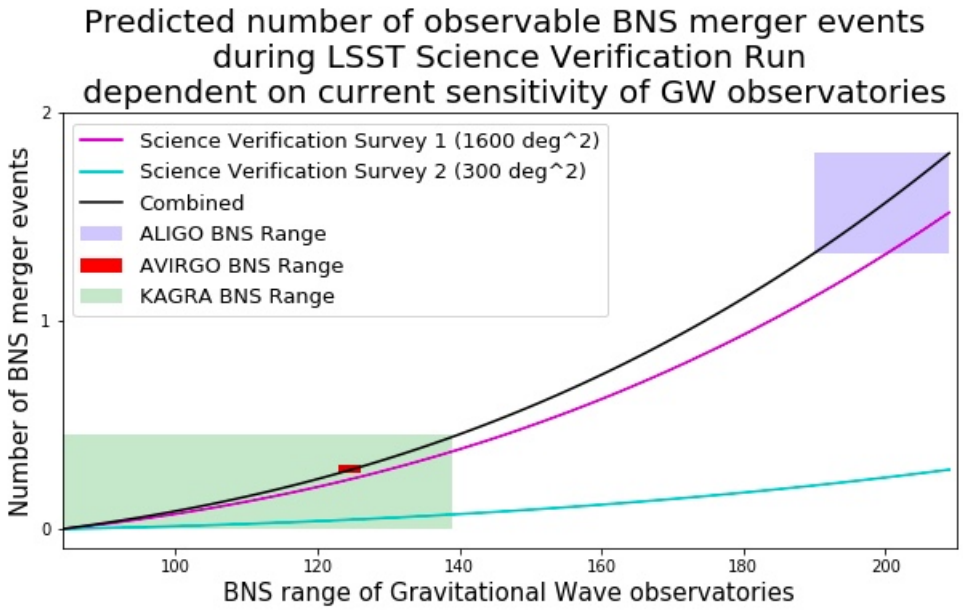

Figure 5: Black line assumed a rate of 10^3 events $\mathrm{Gpc^3 yr^{-1}}$ for BNS merger events. We also assumed LSST would run at design sensitivity during the entire SV period. Predictions assumed a GW observatory duty cycle of 70%. .

of the GW detectors. Assuming a rate of 320 - 4740 BNS events $\mathrm{Gpc^3 yr^{-1}}$ (Abbott et al. 2016), the estimated number of observable events by both aLIGO and LSST during the SV run is about 10 for the most optimistic KAGRA BNS range. This estimate assumes that LSST will be running at design depth during the 80 nights of the SV period and that its field of view will not be restricted to the stated areas in both phases of the run.

3.2 Galaxy catalogs for electromagnetic follow-up of gravitational wave events

Catalogs of galaxies, such as the one build in this work, can also be used in the electromagnetic follow-up of gravitational wave triggers. Section 1.2 described the current strategy to identify and observe BNS mergers with telescopes upon the arrival of a gravitational signal from a candidate BNS merger event. It is critical that the transient is identified and observed as soon as possible, given the fast evolution of the kilonova light curve. Nevertheless, as evidenced by the first observation campaign following the GW170817 event, the process of identifying the source galaxy in the sky presents many difficulties. For instance, LIGO can only provide probability maps for the location of the event, which extend to hundreds of square degrees in the sky. Even with large survey telescopes, observation of those regions in the sky is unfeasible and inefficient.

In this sense, galaxy catalogs can aid the observation campaigns of BNS merger events by providing

a more concise list of candidate source galaxies to a gravitational wave signal. Given that gravitational wave observatories have a finite BNS range for observation, the most probable source galaxies within that distance can be identified and readily imaged. Moreover, a galaxy catalog of this sort will also help in the estimation of cosmological parameters from stardard sirens (described in section 1.4). Cosmological parameter estimation requires an independent measure of redshift to the source galaxy. Such information is contained in galaxy catalogs, either as a photometric or a spectroscopic redshift.

Therefore, the catalog built in this work is not only useful to estimate astrophysical BNS merger rates, but also as a tool to aid during observation campaigns of these events, and in the analysis of observations for cosmological parameter estimation.

4 Conclusion

The method to calculate BNS merger events based on evidence of an r-process event in Reticulum II that scales up with stellar mass yields rates comparable to beam-corrected lower limits to rates of SGRBs in the literature. The two approaches used in this work to estimate the stellar mass in the nearby universe yield very similar results: 285.88 and 266.77 $\mathrm{Gpc}^{-3}\mathrm{yr}^{-1}$ for the Schechter Mass Function and the galaxy catalog approach, respectively. For a 200 Mpc volume, we would expect BNS merger rates of 9.58 yr^{-1} according to the Schechter formalism and 8.93 yr^{-1} from the galaxy catalog estimate. When the nonuniform sensitivity of LIGO for certain of the sky is taken into account, the predicted observable rate in a 200 Mpc volume is 6.3 yr^{-1}.

Future work must be done on using distance-dependent LIGO sensitivity maps to come up with better predictions of observable rates. Moreover, a lower limit to the timescale of BNS mergers should be estimated to further constraint BNS rates. Different methods to calculate the rate of BNS mergers from the event in Ret II could take into account Star Formation Histories and Star Formation Rates to avoid the oversimplification of stellar mass dependent rates.

5 References

Abbott, et al. Phys. Rev. Lett. 119, no. 16 (2017): 18.

Annis, J., et al. Private communication (2015).

Bechtol, K., et al. ApJ 807, no. 1 (2015): 50.

Bell E. F. and de Jong R. S. AJ 550, no. 1 (2001): 212.

Berger, E. Annu. Rev. Astron. Astrophys. 52, no. 1 (August 18, 2014): 43–105.

Chen, H. Y., et al. ApJ 835, no. 1 (2017): 31.

Chen, H. Y. and Holz D. E. Phys. Rev. Lett. 111, no. 18 (October 31, 2013): 181101.

Conselice, C. J., et al. ApJ 830, no. 2 (2016): 83.

Coward, D. M., et al. MNRAS 425, no. 4 (October 1, 2012): 2668–73.

Holz, D. and S.A. Hughes. Ap J 629 (2005): 15.

Drlica-Wagner A., et al. ApJ 813, no. 2 (2015): 109.

Fong, W., et al. Ap J 815, no. 2 (2015): 102.

Ji, A. P., et al. Nature 531, no. 7596 (March 31, 2016): 610–13.

Ji, A. P., et al. ApJ 830, no. 2 (2016): 93.

McConnachie A. W. AJ 144, no. 1 (2012): 4.

Metzger B. D. and Berger E. ApJ 746, no. 1 (2012): 48.

Nissanke S. et al. ApJ 725 (2010): 496.

Rasio, F. A. and Shapiro, S. L., "Coalescing Binary Neutron Stars." Classical and Quantum Gravity 16, no. 6 (1999): R1.

Roederer I. U., et al. AJ 151, no. 3 (2016): 82.

Westmeier, T., R. Braun, and B. S. Koribalski. MNRAS 410, no. 4 (February 1, 2011): 2217–36.